CERTIFICATE

This is to certify that

LEONARDUS SETIA BUDI WIBOWO

Has participated in the First International Forum of Advanced Engineering Technology 2017 (IFAET 2017) as PRESENTER

Organized by

Institut Teknologi Sepuluh Nopember and National Taiwan University of Science and Technology at ITS – Surabaya, Indonesia 19-20th December 2017

Chairman,

IDAA Warmadewanthi,Ph.D
Dean Faculty of Civil, Environmental and Geo Engineering

Co-Chairman,

Prof.Chien-Kuo Chiu
Vice-Dean College of Engineering

CYCLIC BEHAVIORS OF HIGH-STRENGTH RC SQUAT WALLS WITH ASPECT RATIO OF 1.0 AND 1.5

Leonardus S. B. WIBOWO[1] and Min-Yuan CHENG[2]

SUMMARY

This paper evaluates cyclic behaviors of RC squat wall specimens using conventional- and high-strength materials. A total of 4 specimens were tested under lateral displacement reversals. Test parameters include specimen aspect ratio (h_w/ℓ_w), steel grade, and concrete strength. With equivalent steel area force, i.e. total steel area times the steel yield stress, test results indicate specimens using high-strength steel exhibited comparable strength and deformation capacity as specimens using conventional-strength materials. Specimen drift capacity decreases as the normalized shear demand increases. The use of high-strength concrete reduces normalized shear stress demand and results in larger specimen deformation capacity.

Keywords: *strength; deformation; squat wall; high-strength*

INTRODUCTION

Reinforced concrete (RC) shear wall or structural wall has been used extensively as the major lateral-force-resistant system in current practices. For low to mid-rise buildings, a study indicates that using RC shear walls is more cost-effective to resist seismic forces than the RC moment-resisting frames (Moehle et al., 2011). A RC squat wall typically refers to a structural wall having an aspect ratio (h_w/ℓ_w) of 2.0 or less, where h_w is the specimen height and ℓ_w is the specimen length. In regions with high seismicity, the design of RC squat wall in compliance with the specifications of ACI Building Code or ACI 318-14 (ACI Committee 318, 2014) generally results in heavy steel congestion at ends of the wall, where special boundary elements are required. Using high-strength steel may alleviate the steel congestion. However, experimental studies of RC squat walls reinforced with high-strength materials including high-strength steel and high-strength concrete are very limited. A recent publication (Cheng et al., 2016) showed that squat wall specimens using high-strength steel with specified yield strength, f_y, above 685 MPa exhibited comparable strength and deformation capacity as specimens using conventional Grade 60 (413 MPa) steel, providing that specimens were designed with a similar shear stress demand associated with development of the flexural strength at the wall base. In that study, however, all test specimens had an aspect ratio of 1.0 and concrete strength, f_c', of around 41 MPa.

This study aims to extend the existing test results. Focus is given on walls with shear stress demands approaching $0.83\sqrt{f_c'(\text{MPa})}$ because walls with such high shear demand appear to be more critical for strength and deformation capacities (Cheng et al., 2016). A total of 4 specimens were tested under lateral displacement reversals. Primary test parameters include (1) specimen aspect ratios, (2) steel grade, and (3) concrete strength. A test matrix that presents these key test parameters in each test specimen is summarized in Table 1. In which, V_{n1} and V_{n2} is the nominal shear capacity determined based on Eq. 1, and Eq. 2, respectively, per ACI 318-14. In which, A_{cv} is the wall cross section area determined by wall width (b_w) times the wall length (ℓ_w), and ρ_t is the horizontal web reinforcement ratio.

[1] PhD student, National Taiwan University of Science and Technology, Taiwan, e-mail: bowobudi84@gmail.com
[2] Associate Professor, National Taiwan University of Science and Technology, Taiwan, e-mail: minyuancheng@mail.ntust.edu.tw

$$V_{n1} = A_{cv}\left(0.25\sqrt{f'_c} + \rho_t f_y\right) \le 0.83\sqrt{f'_c}A_{cv}, \text{ MPa} \qquad \text{Eq. (1)}$$

$$V_{n2} = 0.6A_{vf}f_y \le \min\left(0.2f'_c A_{cv}, \left(3.3 + 0.08f'_c\right)A_{cv}, 11A_{cv}\right), \text{ MPa} \qquad \text{Eq. (2)}$$

Table 1 - Design Parameters for Test Specimens

Specimens	$\frac{h_w}{\ell_w}$	**Vertical Reinforcement Grade in SBE*, MPa**	**Web Reinforcement Grade, MPa**	**Confinement Reinforcement Grade, MPa**	**Specified Concrete strength f'_c, MPa**	$\frac{V_{mpr}}{A_{cv}\sqrt{f'_c}(\text{MPa})}$	$\frac{V_{n1}}{V_{mpr}}$	$\frac{V_{n2}}{V_{mpr}}$
(1)	(2)	(3)	(4)	(5)	(6)	(7)	(8)	(9)
HHH_1.0	1.0	785	785	785	69	0.61	1.07	1.13
CCC_1.5	1.5	413	413	413	41	0.77	1.02	1.80
HCC_1.5	1.5	685	785	413	41	0.81	0.94	1.82
HHH_1.5	1.5	685	785	785	69	0.65	0.99	1.75

* SBE: special boundary element.

EXPERIMENTAL PROGRAM

Test Specimens

Each specimen consists of three parts including a top concrete block, the wall section, and a concrete base block. The top concrete block was designed for lateral load application, and the concrete base lock was designed to provide the fixed boundary condition at base of the wall. Reinforcement layouts of the wall sections are presented in Fig. 1. Longitudinal reinforcement of specimens CCC_1.5 and HCC_1.5 were designed to have shear stress demand, V_{mpr}/A_{cv}, close to $0.83\sqrt{f'_c}$ (MPa), as shown in column (7) of Table 1. In which, V_{mpr} is calculated using the probable flexural strength, M_{pr}, divided by the specimen height, h_w. For specimens using Grade 60 and high-strength (USD685 or USD785) steel, M_{pr} is determined based on 1.25 and 1.20 specified steel yield strength, respectively.

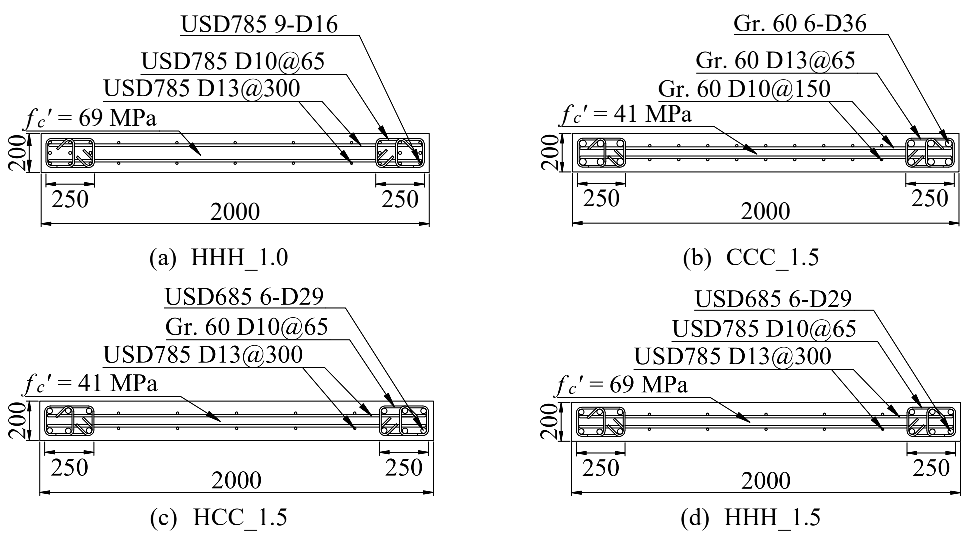

(a) HHH_1.0 (b) CCC_1.5

(c) HCC_1.5 (d) HHH_1.5

Fig. 1 – Reinforcement Layout (unit : mm)

Horizontal web reinforcement was provided such that the shear capacity per Eq. 1 is approximately equal to the shear demand, i.e. $V_{n1} \cong V_{mpr}$, as shown in column (8) of Table 1. Specimen HHH_1.5 was designed to have the same reinforcement layout as specimen HCC_1.5. As a result, the normalized shear stress demand, i.e. $V_{mpr}/\left(A_{cv}\sqrt{f'_c}\right)$, is slightly reduced. Please note, reinforcement layout of specimen HHH_1.0 is based on that of specimen H115 from the previous study (Cheng et al., 2016). All specimens had No. 3 confinement reinforcement spaced at 65 mm in the special boundary elements to satisfy the required spacing controlled by one-third of the wall thickness and required area per ACI 318-14.

Experimental Setup and Instrumentations
The experimental setup is shown in Fig. 2. This setup intends to impose in-plane single-curvature deformation to the test specimens with negligible axial force.

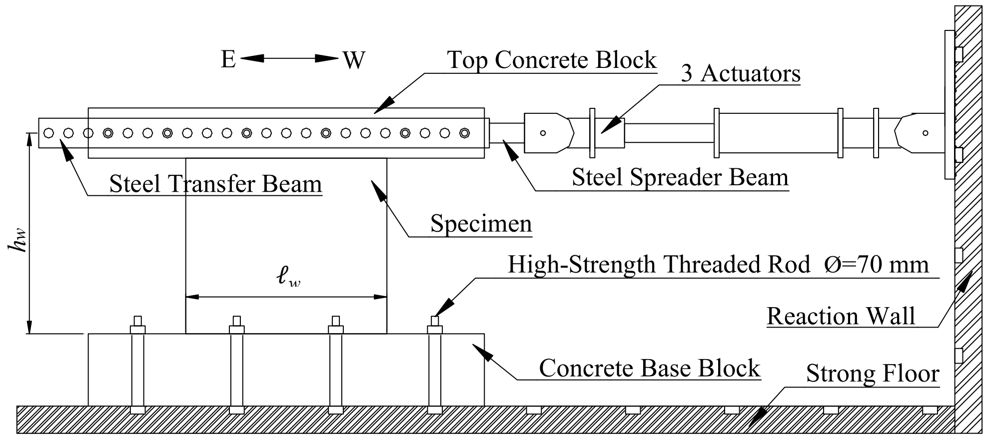

Fig. 2 - Test Setup

EXPERIMENTAL RESULTS

Overall Response
Inclined and horizontal cracks developed in all test specimens during the 1st cycle at 0.25% target drift level. Spalling of concrete cover for specimen HHH_1.0 was first observed at the extreme compression fiber during the 1st cycle of 1.50% target drift. In the 2nd cycle, some spalling of cover concrete was also found at lower part of the web region close to the edge of special boundary element. After that, damage continuously accumulated at lower part of the wall within a distance of 300 mm approximately from the face of concrete base block. During the 2.00% target drift cycles, severe concrete deterioration resulted in apparent sliding at the wall base.

For specimens CCC_1.5 and HCC_1.5, only a small portion of concrete cover within the lower part of the special boundary element (not at extreme compression fiber) showed signs of distress after completion of the 1.00% target drift cycles. At the same target drift level, concrete distress was not that clear in specimen HHH_1.5. During the 1.50% target drift cycles, severe concrete deterioration in the lower part of the wall was observed in specimens CCC_1.5 and HCC_1.5 but in different ways. As can be seen from Fig. 3(b) and Fig. 3(c), Due to this concentration of damage, a triangle piece was gradually formed at base of the wall and this piece appeared to reduce the sliding deformation in specimen HCC_1.5, Fig. 3(c). For specimen CCC_1.5, on the other hand, sliding was very apparent in the 2nd and 3rd cycle of 1.50% target drift. For specimen HHH_1.5, only slight spalling of cover concrete was observed at the end of 1.50% target drift cycles. Concrete deterioration at lower part of the wall became gradually severe during the 2.00% target drift cycles for specimen HHH_1.5. Despite that concrete deterioration at the wall base was observed at different drift level, as can be seen from Figs. 3(c) and 3(d), specimens HCC_1.5 and HHH_1.5 appear to have a similar failure mode.

(a) HHH_1.0

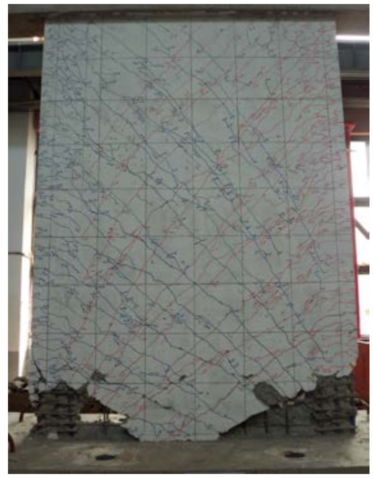

(b) CCC_1.5

(c) HCC_1.5

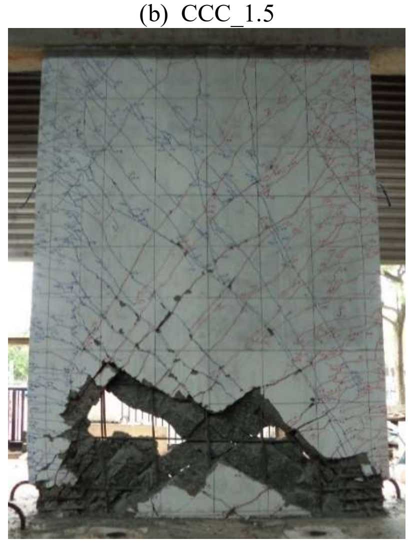

(d) HHH_1.5

Fig. 3 – Final States of Test Specimens

Test Results

Material test results are listed in Table 2. Hysteretic responses of all specimens are presented in Fig. 4. Please note that the drift presented in Fig. 4 and later in this paper deviates from the target value due to adjustments for lateral movement and rotation of the concrete base block. Key test results are summarized in Table 3. Ultimate drift ratio d_u is defined at the point when one of the following two criteria is first met: 1) the drift where the load drops 20% from the peak on the envelope curve; or 2) the drift where the load drops more than 20% in the repeated cycles and the load in the 1st cycle of the next drift level is lower than the load in the 3rd cycle of this drift level. The loading direction in which d_u is determined is consistent with that of V_{peak}, the larger peak strengths from the two loading directions.

Table 2 - Summary of Concrete Cylinder Strength and Reinforcement Properties

Specimen name	Vertical Reinforcement in SBE*, MPa		Web Reinforcement, MPa		Confinement Reinforcement, MPa		Concrete Cylinder Strength, MPa
HHH_1.0	D16	877	D13	883	D10	908	75.2
CCC_1.5	D36	462	D13	465	D10	480	43.2
HCC_1.5	D29	707	D13	870	D10	480	39.7
HHH_1.5	D29	707	D13	870	D10	868	101

* SBE: special boundary element.

Table 3 - Summary of Test Results and Shear Strength Evaluation

Specimen name	V_{peak}, kN	$\frac{V_{peak}}{A_{cv}\sqrt{f'_c}(\text{MPa})}$	d_u (%)	$\frac{V_{peak}}{V_{mn}}^{(1)}$	$\frac{V_{peak}}{V_{mpr}}^{(2)}$	$\frac{V_{peak}}{V_{n1}}^{(3)}$	$\frac{V_{peak}}{V_{n2}}^{(3)}$
HHH_1.0	1939	0.56	1.93	1.02	0.95	0.83	0.75
CCC_1.5	1882	0.72	1.46	1.02	0.84	0.85	0.47
HCC_1.5	1841	0.73	1.45	1.00	0.90	0.89	0.47
HHH_1.5	2082	0.52	1.96	1.08	0.96	0.85	0.53

(1) V_{mn} is the shear demand associated with development of nominal flexural capacity at the wall base using tested material properties.

(2) V_{mpr} is the shear demand associated with development of the probable flexural capacity, M_{pr}, at base of the wall using concrete cylinder strength and 1.25 specified yield strength for Grade 60 steel but 1.20 specified yield strength for USD685 and USD785 steels.

(3) V_{n1} and V_{n2}, are determined based on tested material strength.

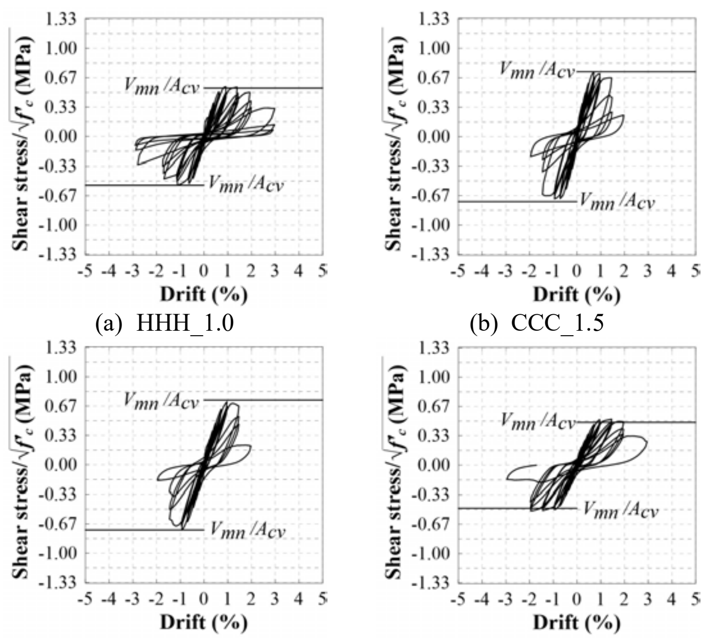

(a) HHH_1.0 (b) CCC_1.5

(c) HCC_1.5 (d) HHH_1.5

Fig. 4 – Specimen Hysteretic Responses

-Strength

As can be seen from Table 3, V_{peak} for specimens with aspect ratios of 1.0 or 1.5 can be satisfactorily estimated by V_{mn}, the shear demand associated with development of the nominal flexural strength (M_n) at the wall base, i.e. $V_{mn} = M_n/h_w$. In addition, V_{mpr} corresponding to the probable moment strength, M_{pr}, achieved at the wall base, i.e. $V_{mpr} = M_{pr}/h_w$, provides a satisfactory upper bound for V_{peak}. Please note, M_n is determined using tested material properties, while M_{pr} is determined using concrete cylinder strength with 1.25 and 1.20 specified yield strength for Grade 60 and high-strength steel (USD685/USD785), respectively.

Specimen peak strengths are also evaluated using two shear strength models. The first strength model is based on Eq. 1 per ACI 318-14 and its value is denoted as V_{n1}. The second strength model denoted as V_{n2} is based on Eq. 2. Both shear strength models overestimated the peak strength, likely because specimens peak strength is limited by flexural. Specimens using high-strength steel (either USD685 or USD785) exhibited comparable V_{peak} as specimens using conventional Grade 60 steel, providing that the steel area force, i.e. total steel area times the steel yield strength, in the specimens is equivalent. Increasing concrete strength increases V_{peak} slightly.

-Deformation

Previous researches indicate that the wall deformation capacity increases as the normalized shear demand decreases (Cheng et al., 2016; Athanasopoulou and Parra-Montesinos, 2013). The normalized shear stress demand versus ultimate deformation capacity, d_u, for all specimens is presented in Fig. 5. Test specimens from the current study and the two specimens from the previous research (Cheng et al., 2016) are collectively presented in the figure with a superscript asterisk. These two specimens both had normalized shear stress demand of around $0.67\sqrt{f_c'(\text{MPa})}$ and aspect ratio of 1.0.

As can be seen from Fig. 5, the trend shows that specimen deformation capacity increases as the normalized shear demand decreases. Increasing concrete strength to reduce the normalized shear stress demand improves specimen deformation capacity.

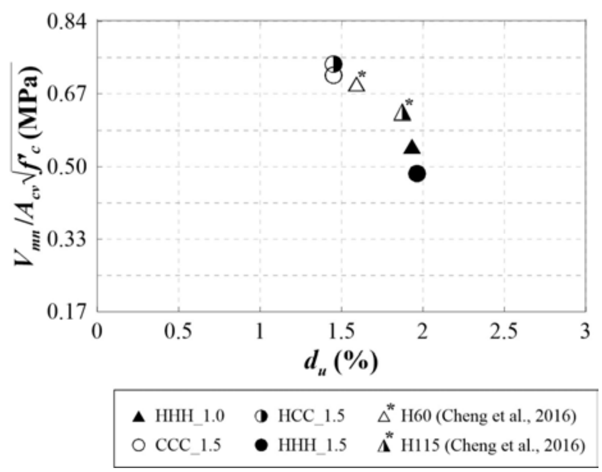

Fig. 5 – Nominalized Shear Stress versus Deformation Capacity

PRELIMINARY CONCLUSION

This study extends the work from a previous research (Cheng et al., 2016) by testing another four RC squat wall specimens using conventional and high-strength materials. Test parameters include specimen aspect ratio, steel grade, and concrete strength. Based on test results, the following conclusions are drawn:

(1) Specimens using high-strength steels exhibited comparable strength as specimens using conventional Grade 60 steels with equivalent steel area force, i.e. total steel area times the steel yield stress.
(2) Peak strengths of specimens with aspect ratio of 1.0 and 1.5 can be reasonably estimated by the nominal flexural strength.
(3) Specimen deformation capacity decreases as the normalized shear demand associated with development of the nominal flexural strength increases. The use of high-strength concrete results in lower shear stress demand and larger specimen deformation capacity.

REFERENCES

ACI Committee 318, (2014), "Building Code Requirements for Structural Concrete and Commentary (ACI 318-14)," American Concrete Institute, Farmington Hills, Michigan, 519 pp.

Athanasopoulou, A. and Parra-Montesinos, G., (2013), "Experimental Study on the Seismic Behavior of High-Performance Fiber-Reinforced Concrete Low-Rise Walls," ACI Structural Journal, V. 110, No.5, Sep.- Oct., pp. 767-778.

Cheng, M-. Y.; Hung, S-. H.; Lequesne, R. D.; and Lepage, A., (2016), "Earthquake-Resistant Squat Walls Reinforced with High Strength Steel," ACI Structural Journal, V. 113, No.5, Sep.- Oct., pp. 1065-1076.

Moehle, J. P.; Ghodsi, T.; Hooper, J. D.; Fields, D. C.; and Gedhada, R., (2011), "Seismic Design of Cast-in-Place Concrete Special Structural Walls and Coupling Beams: A Guide for Practicing Engineers," National Institute of Standards and Technology, pp. 37.